A NOVEL PHOTONIC DEW-POINT HYGROMETER WITH ULTRA-HIGH ACCURACY

Jifang Tao[1], Li Wang[2], Hong Cai[1], Tao Sun[1], Junfeng Song[1], and Yuandong Gu[1†]
[1]Sensors & Actuators Microsystems Program, Institute of Microelectronics, Agency of Science, Technology and Research (A*STAR), 11 Science Park Road, 639798, SINGAPORE
[2]Temperature & Humidity Laboratory, National Metrology Center, A*STAR, 1 Science Park Drive, 118221, SINGAPORE

ABSTRACT

Dew-point is the temperature at which vapor begins to condense out of the gaseous phase. The deterministic relationship between dew-point temperature and relative humidity brought about the industry widely-accepted "chilled-mirror" dew-point hygrometers for highly accurate humidity measurement, essential for a broad range of industrial and metrology applications, despite several limitations such as high cost, large size and slow response. In this report, we demonstrate a compact, integrated photonic dew-point hygrometer that features ultra-high accuracy (potential +/- 0.02), small footprint (~ mm^2), and fast response (< 1 minute), which paves the way for high accuracy on-chip dew-point detection; promises broader adoption in applications which conventional technology is unsuitable due to size, cost, and other constraints.

INTRODUCTION

Real-time and precise measurement of relative humidity is of great importance in modeling of global warming and weather changes [1-2]. It also has wide applications, including aero engine acoustic testing, accurate natural gas metering, in-door air quality (IAQ) and breathing gases monitoring, etc [3-9]. Many types of humidity sensors or hygrometers have been developed over the years. The common cost-effective miniaturize solutions are achieved by employing a solid-state sensing film that interacts with water vapor and converts water vapor concentration into an electrical signal, such as capacitance or resistance [10]. These electronic humidity sensors have the universal shortcoming of drift and contamination induced inaccuracy, which limits their accuracy in the typical range of +/-1% to +/-5%, which could further degrade in low relative humidity (0 ~ 20%) and high relative humidity (80% ~ 100%) environment. For applications that require higher accuracy, industry employs "chilled-mirror" dew-point hygrometer, in which a polished mirror is cooled by a thermoelectric cooler and a platinum resistance thermometer (PRT) is imbedded within the mirror surface to measure its surface temperature. An electro-optic detection system, which consists of a light-emitting diode (LED) and a light detector, is used to monitor fine water droplets condensed at mirror surface by detecting the reduction in the reflected light caused by water droplets which induce scattering. Its accuracy in dew-point temperature measurement is typically +/- 0.1 °C over a wide temperature span, which means the relative humidity accuracy is up to +/- 0.01% when relative humidity is around 1% and environmental temperature is 25°C [11]. However, its high price (up to US$50,000), large footprint (> 4000 cm^3), and slow response (in minutes), particularly for lower dew-point temperatures, limit its wide adoptions. And in some high-end applications, such as aerospace and metrology centers, the accuracy of +/- 0.1°C is still cannot fully meet the requirements. To achieve higher accuracy, it is also challenging due to many types of temperature errors, e.g. temperature error due to self-heating and measurement hysteresis of the embedded thermometer. Although some potentially disruptive solutions based on carbon nanotubes or grapheme have been reported with a high sensitivity, they suffered from particles/gas molecules-induced interference inevitably [12-13]. Integrated photonics technology has matured over the past decades, providing a miniaturize, high sensitive detecting, and cost-effective platform for on-chip sensing [14-15]. Here, we show a general approach to design a novel dew-point hygrometer based on integrated photonics technology.

DESIGN & FABRICATION

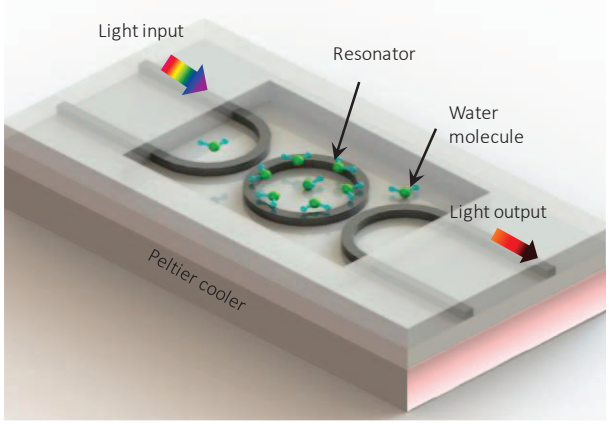

Figure 1: 3D illustration of integrated photonic dew-point hygrometer. The photonic micro-ring resonator acts "chilled-mirror" and "thermometer" simultaneously.

The schematic of the proposed miniature dew-point hygrometer is shown in Fig. 1, in which a partially exposed photonic micro-ring resonator chip is placed on top of a Peltier cooler. It cools the chip down to below dew-point temperature imperceptibly. The micro-ring resonator supports some high quality-factor (Q-factor) resonance modes whose frequencies are susceptible to the change of the dielectric properties of the surrounding medium. In our design, the micro-ring resonator serves two functions simultaneously: 1) senses the condensed water droplets via evanescent fields, and 2) functions as a highly accurate, *in-situ* temperature sensor via thermo-optic effect (TOE). When the chip is cooled down to the dew-point

temperature, water droplets will condense at the top surface of the resonator. The condensed water droplets has higher refractive index than the air surrounding the micro-ring resonator, which results in a significant shift of the resonant wavelengths of the micro-ring resonator. By recording the wavelength changes, the dew-point temperature can be interpreted.

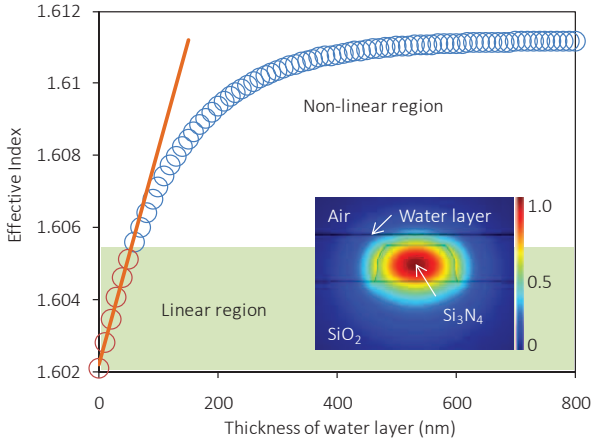

Figure 2: Simulation of the effective index changes vs. the thickness of water layer. Inset is finite element simulation result showing the E_x component of the optical fields. The evanescent-field ratio is around 4.1% at air.

The effective index of the micro-ring resonator increases with the water layer thickness, as shown in Fig. 2. The energy of the evanescent wave of the fabricated Si_3N_4 waveguide accounts for around 4.1% of the total photonic energy based on the simulation as shown in the insert. The effective index of the water layer increases almost linearly with the thickness when the water layer thickness is below 50 nm. When water layer increases continuous, the effective index increasing rate becomes slow due to the gradient decreasing evanescent filed at outside of waveguide. This forms the foundation of the linear fitting for subsequent dew-point temperature extraction.

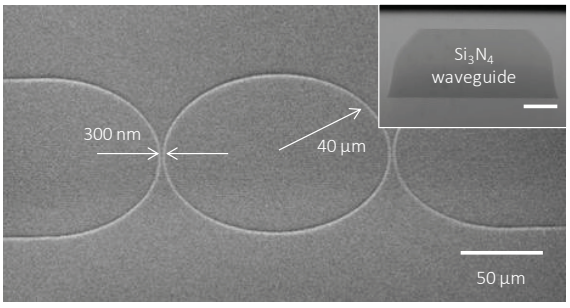

Figure 3: SEM of the photonic chip based on Si_3N_4 waveguides. Insert shows the cross-section of the Si_3N_4 waveguide, with a dimension of 1-µm width and 0.4-µm height.

Figure 3 shows the SEM of the micro-ring resonator with a 40-µm radius and a 300-nm coupling gap between the input/output waveguide and the micro-ring resonator. Chip fabrication starts with a 3.5-µm thick thermal silicon dioxide (SiO_2) layer and a 400-nm thick silicon nitride (Si_3N_4) layer deposition in a low pressure chemical vapor deposition (LPCVD) furnace. Followed by waveguide structures defined using deep UV photolithography. Reactive ion etching (RIE) is used to transfer waveguide patterns onto the Si_3N_4 layer. The second RIE dry etch is performed to remove waveguide edges to minimize the optical transmission loss as shown in insert. An 800-nm SiO_2 cladding layer is blanket deposited on the entire device structure by plasma-enhanced chemical vapor deposition (PECVD). Finally, a chemical mechanical polishing (CMP) process is used to thin down the cladding SiO_2 layer to 120 nm. The CMP process provides a pristine surface for water molecule condensation.

EXPERIMENTAL RESULTS

In the experiments, a light beam from a broadband light source is coupled into the photonic chip, which in turn generates a periodic resonant wavelength spectrum. A selected output resonant wavelength (λ_r) value is recorded by a wavelength meter in real-time. Here we highlight that an almost linearly spectral shift response upon the temperature change is obtained over the temperature range of -30 °C to 60 °C with a sensitivity of ~37 pm/°C, as shown in Fig.4. Insert shows the transmission spectrum responding to temperature at -20 °C, 0 °C and 20 °C. The Q-factor of up to 24,000 of the micro-ring resonator at around 1589 nm is achieved. And the waveguide propagation loss is only 0.34 dB/cm.

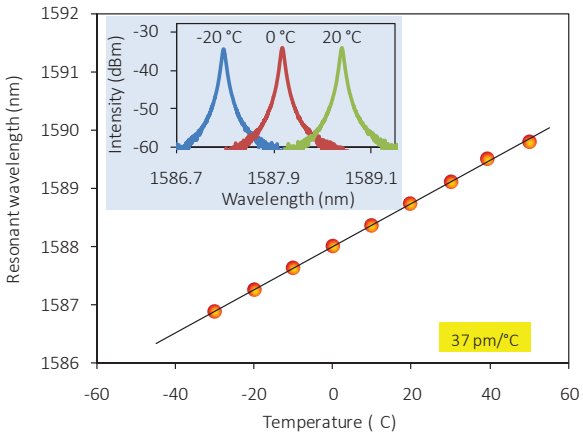

Figure 4: Linear spectral shift of the micro-ring resonator in response to the temperature change, with a sensitivity of 37 pm/°C. Insert shows transmission spectrum responding to temperature change.

A typical spectrum response of the micro-ring resonator in dew-point temperature detection process is shown in Fig. 5. The dew-point temperature and ambient temperature of the testing air are 20 and 25 °C, respectively. Before the chip temperature reaches the dew-point temperature, the resonant wavelength is blue-shifted as the temperature is decreasing (blue line in Fig. 5). When the chip is cooled down to the dew-point temperature, water molecules start to condense on the surface of the chip. These water molecules eventually increase the effective index of the micro-ring resonator abruptly because of the higher refractive index of water

(n_{water} = 1.32, n_{air} = 1). As a result, the resonant wavelength of the micro-ring resonator is red-shifted (red line in Fig. 5). By fitting the resonant wavelength value measured in these two progresses separately, an intersection is obtained which depicts the dew-point temperature and time at which dew starts to be generated is depicted, as shown in Fig. 5. It measures the temperature when dew starts, i.e., dew-point temperature. The green line and dark blue line denote the progress of water droplets evaporation and temperature returning to its original status, respectively. The time-consuming in the intersection point obtaining (blue line and red line in Fig. 5) is less than 30 seconds. It will be longer when the dew-point temperature is lower. However, this time consumption is much shorter than conventional approaches due to small thermal mass. More reliable measurement can be done through repeated cycles in a reasonable short time, because the temperature is not necessary to return its original status and the ambient temperature can be monitored by using a separate resonator. With the unique feature of the micro-ring resonator, ambient temperature and dew-point temperature can be extracted from the spectra. Thus, external thermometer and complex temperature management system can be avoided.

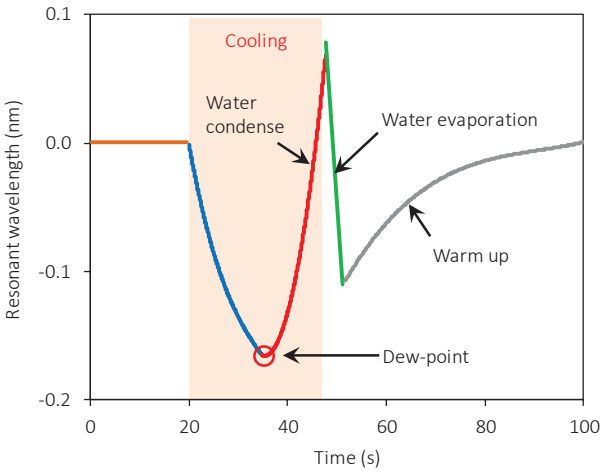

Figure 5: Typical wavelength response cycle of the micro-ring resonator, from (TEC on) cooling without condensation and condensation, (TEC off) water droplets evaporation and warming up.

To evaluate the performance of the device, dew-point temperatures ranging from -20 °C to 20 °C were obtained. In the experimental setup, the photonic chip is placed into a metal chamber which connects with a reference humidity generator (Thunder Scientific Model 4500) which generates nitrogen gas with known dew-point temperature. During the measurement, the gas passed through the metal chamber at a constant flow rate. The results are depicted by blue circles in Fig. 6. A good linear fitting line for the relationship between dew-point temperature and resonant wavelength changes were obtained. Some forecasted resonant wavelengths are plotted by black open circles in Fig. 6. It is notable that photonic devices without doping process are very stable at low temperature indicating promises that a wider dew-point temperature detection range can be achieved by use of a more powerful thermoelectric cooler. Based on the values of ambient temperature and dew-point temperature measured by the photonic chip, the corresponding relative humidity value can be calculated directly by use of the formula as depicted by orange squares in Fig. 6 [16]. It covers relative humidity range from 0% to 100%. At low relative humidity environment, the curve has a small slope which means a better resolution can be obtained, which is a challenging region for most of miniaturize humidity sensors.

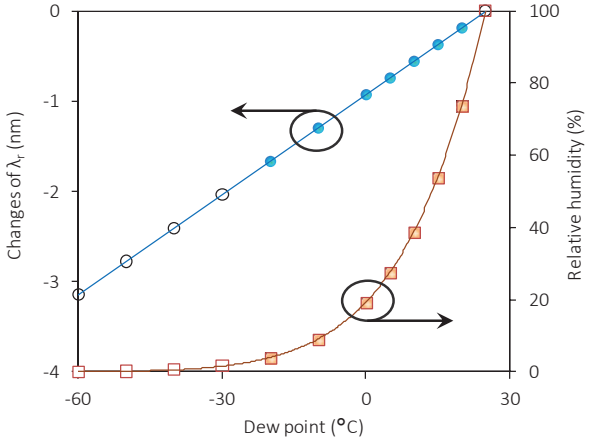

Figure 6: Measured relationship between dew-point temperature and relative humidity vs. wavelength changes. Dew-point temperature is correlates linearly with resonant wavelength shift. And relative humidity is calculated based on dew-point and ambient temperatures.

A chilled-mirror dew-point hygrometer suffers intrinsic errors mainly induced by 1) temperature gradient from mirror surface to the embedded thermometer; 2) thermal conductance of the thermometer leads; 3) self-heating of the thermometer. These errors set practical limits of its measurement accuracy at around +/- 0.1 °C. This reported integrated photonic dew-point hygrometer uses a single sensing element, the micro-ring resonator, to detect both water condensation process and the corresponding temperatures simultaneously. This virtually integrates the chilled-mirror and the thermometer together, eliminating errors induced by temperature gradient, thermal conductance and self-heating. Its potential accuracy can be greatly improved.

CONCLUSIONS

A novel photonic dew-point hygrometer has been developed based on integrated photonics technology for highly sensitive dew-point temperature and relative humidity detection, taking advantage of the thermo-optics effect and the evanescent field sensing. Superior performance including high accuracy and fast response has been achieved on a miniaturize silicon chip. This photonic dew-point hygrometer paves the way for on-chip dew-point detection, and promises broader applications for accurate and reliable humidity measurement in aerospace, meteorology, petrochemical, agriculture, biology, and pharmaceutics.

REFERENCES

[1] S.-i. Ohkoshi, K.-i. Arai, Y. Sato, and K. Hashimoto, "Humidity-induced magnetization and magnetic pole inversion in a cyano-bridged metal assembly," *Nat. Mater.*, vol. 3, pp. 857-861, 2004.

[2] E. M. Fischer, and R. Knutti, "Robust projections of combined humidity and temperature extremes," *Nat. Clim. Change*, vol. 3, pp. 126-130, 2013.

[3] N. Herzer, H. Guneysu, D. J. D. Davies, D. Yildirim, A. R. Vaccaro, D. J. Broer, C. W. M. Bastiaansen, and A. P. H. J. Schenning, "Printable optical sensors based on H-bonded supramolecular cholesteric liquid crystal networks," *J. Am. Chem. Soc.*, vol. 134, pp. 7608-7611, 2012.

[4] Q. Xue, H. Chen, Q. Li, K. Yan, F. Besenbacher, and M. Dong, "Room-temperature high-sensitivity detection of ammonia gas using the capacitance of carbon/silicon heterojunctions," *Energy Environ. Sci*., vol. 3, pp. 288-291, 2010

[5] Y. Zhang, K. Yu, D. Jiang, Z. Zhu, H. Geng, L. Luo, "Zinc oxide nanorod and nanowire for humidity sensor," *Appl. Surf. Sci.*, vol. 242, pp. 212-217, 2005.

[6] Q. Kuang, C. Lao, Z. L. Wang, Z. Xie, L. Zheng, "High-sensitivity humidity sensor based on a single SnO2 nanowire," *J. Am. Chem. Soc*., vol. 129, pp. 6070-6071, 2007.

[7] H. Nakagawa, S. Okazaki, S. Asakura, K. Fukuda, H. Akimoto, S. Takahashi, S. Shigemori, "An automated car ventilation system," *Sens. Actuators B*, vol. 65, pp. 133-137, 2000.

[8] U. Mogera, A. A. Sagade, S. J. George, and G. U. Kulkarni, "Ultrafast response humidity sensor using supramolecular nanofiber and its application in monitoring breath humidity and flow," *Sci. Rep.*, vol. 4, 4103, 2014.

[9] G. Mattana, T. Kinkeldei, D. Leuenberger, C. Ataman, J. J. Ruan, F. Molina-lopez, A. Vasquez Quintero, G. Nisato, G. Troster, D. Briand, N. F. de Rooij, "Woven temperature and humidity sensors on flexible plastic substrates for E-textile applications," *IEEE Sens*., vol. 13, 2013.

[10] C-L. Dai, "A capacitive humidity sensor integrated with micro heater and ring oscillator circuit fabricated by CMOS-MEMS technique," *Sens. Actuators B,* vol. 122, pp. 375-380, 2007

[11] P. R. Wiederhold, Water vapor measurement – methods and instrumentation. Marcel Dekker Inc, New York, 1997.

[12] P. Wang, F. Gu, L. Zhang, L. Tong, "Polymer microfiber rings for high-sensitivity optical humidity sensing," *Appl. Opt.*, vol. 50, G7-G10, 2011.

[13] W. P. Chen, Z. G. Zhao, X. W. Liu, Z. X. Zhang, C. G. Suo, "A capacitive humidity sensor based on multi-wall carbon nanotubes (MWCNTs)," *IEEE Sens.*, vol. 9, pp. 7431-7444, 2009.

[14] J. F. Tao, H. Cai, Y. D. Gu. J. Wu, A. Q. Liu, "Demonstration of a photonic-based linear temperature sensor," *IEEE Photonics. Technol. Lett.*, vol. 27, pp. 767-769, 2015.

[15] J. F. Tao, H. Cai, Y. D. Gu, A. Q. Liu, "Demonstration of a compact wavelength tracker using a tunable silicon resonator," *Opt. Express*, vol. 22, pp. 24104-24110, 2014.

[16] M. G. Lawrence, "The relationship between relative humidity and the dewpoint temperature in moist air: a simple conversion and applications," *Bull. Amer. Meteor. Soc.*, vol. 86, pp. 225-233, 2005

CONTACT

[†]Y. D. Gu, Tel: +65 6770 5915; guyd@ime.a-star.edu.sg